A Description of the Air Force Real-Time Nephanalysis Model

THOMAS M. HAMILL*

Meteorological Models Section, Air Force Global Weather Central, Offutt AFB, Nebraska

ROBERT P. D'ENTREMONT AND JAMES T. BUNTING

Satellite Meteorology Branch, Geophysics Directorate, Phillips Laboratory, Hanscom AFB, Massachusetts

(Manuscript received 24 February 1991, in final form 6 February 1992)

ABSTRACT

The Air Force Global Weather Central (AFGWC) Real-Time Nephanalysis (RTNEPH) is an automated cloud model that produces a 48-km gridded analysis of cloud amount, cloud type, and cloud height. Its primary input is imagery from polar-orbiting satellites.

Six main programs make up the RTNEPH. These are the satellite data mapper, the surface temperature analysis and forecast model, the satellite data processor, the conventional data processor, the merge processor, and the bogus processor. The satellite data mapper remaps incoming polar-orbiter imagery to a polar-stereographic database. The surface temperature model produces an analysis and forecast of shelter and skin temperatures for comparison to satellite-measured infrared (IR) brightness temperatures. The satellite data processor reads in the new satellite data and produces a satellite-derived cloud analysis. The conventional data processor retrieves and reformats cloud information from airport observations. The merge processor combines the satellite- and conventional-derived cloud analyses into a final nephanalysis. Finally, the bogus processor allows forecasters to manually correct the nephanalysis where appropriate.

The RTNEPH has been extensively redesigned, primarily to improve analyses of total and layered cloud amounts generated from IR data. Recent enhancements include the use of regression equations to calculate atmospheric water vapor attenuation, an improved definition of surface temperatures used to calculate cloud/no-cloud thresholds for IR data, and the use of Special Sensor Microwave/Imager (SSM/I) data to further improve the calculation of infrared cloud/no-cloud thresholds. Planned enhancements include the processing of geostationary satellite data, more sophisticated processing of visible data, and a higher-resolution satellite database for the archiving and processing of multispectral satellite data.

1. Introduction

The Real-Time Nephanalysis (RTNEPH) is a cloud analysis model generated at the Air Force Global Weather Central (AFGWC), Offutt Air Force Base, Nebraska. Most of the data analyzed by the RTNEPH comes from Defense Meteorological Satellite Program (DMSP) satellites, though conventional cloud observations and some NOAA polar-orbiting satellite data are used. The RTNEPH data are archived in a polar-stereographic database storing total and layered cloud amounts, cloud bases and tops, and cloud types at 48-km (25-n mi) resolution true at 60°N and S latitude. The RTNEPH became operational in August 1983, replacing the 3-Dimensional Nephanalysis Model (3DNEPH), which had been running since 1970.

The RTNEPH may be used in numerical weather prediction (NWP) applications, including analysis/initialization of cloud or moisture fields, development of cloud forecast parameterization schemes, and verification of cloud forecast fields. The RTNEPH and its predecessor, the 3DNEPH, were created for one such purpose, the initialization of trajectory-based cloud forecast models run at AFGWC (Crum 1987). These cloud forecasts are used for a variety of purposes, including forecasts for aviation. Subsequently, the RTNEPH is also used to verify these cloud forecasts.

In a more conventional data-assimilation system, Norquist (1988) and Nehrkorn and Hoffman (1990) demonstrated the use of RTNEPH/3DNEPH data to improve moisture analyses. In such an application, the RTNEPH cloud amounts are empirically converted, layer by layer, to humidity estimates to provide humidity observations to an analysis scheme. Thereby, in regions with sparse conventional data, the RTNEPH can help delineate areas of high relative humidity. This can potentially improve the short-term latent heating processes in numerical forecasts and help correct the

* *Current affiliation and corresponding author address:* Thomas M. Hamill, Atmospheric and Environmental Research, Inc., 840 Memorial Dr., Cambridge, MA 02139.

"spinup" problem of precipitation deficits during the first few hours of numerical integrations (Mohanty et al. 1986; Lejenas 1979).

In medium-range weather forecasts, numerical models are somewhat insensitive to initial moisture conditions in the extratropics. However, longer-range forecasts need accurate cloud parameterization schemes to faithfully calculate the global distribution of solar and longwave radiative fluxes. Two well-known cloud schemes are the prognostic scheme of Sundqvist et al. (1989) and the diagnostic scheme of Slingo (1987). Slingo showed that unduly simple parameterizations of clouds can lead to a weakening of the extratropical circulation in medium-range forecasts, particularly at the synoptic scale. Mitchell and Hahn (1989) demonstrated how, for any given numerical model, the RTNEPH can be used to tune humidity thresholds common in diagnostic cloud schemes to yield virtually no bias in forecast cloud amount. The National Meteorological Center (NMC) has been acquiring the RTNEPH in real time, four times daily since June 1991, to pursue a number of the above applications of gridded cloud analyses (Campana et al. 1991).

Clouds play an even more important role in climate modeling. Integrated over extended periods of time and large areas, small variations in cloud cover, especially low cloud, can have dramatic influences on surface temperatures (Schneider 1972). For climate applications, the International Satellite Cloud Climatology Project (ISCCP) provides a dedicated database of cloud parameters at 250-km resolution (Rossow et al. 1985; Schiffer and Rossow 1985).

ISCCP data has advantages as well as disadvantages when compared against RTNEPH data. ISCCP data may be more useful than the RTNEPH in the following respects. First, the RTNEPH lacks estimates of cloud optical properties. Second, frequent improvements have been made to the RTNEPH over the past seven years, so the RTNEPH is less useful for year-to-year comparisons of cloud cover. Finally, the RTNEPH is not updated as many times per day as the ISCCP database, since the RTNEPH is currently constrained by the temporal limitations imposed as a consequence of using DMSP data. These satellites are in a polar orbit, and with a constellation of only two satellites, this guarantees most points will be updated four times in a 24-h period; the ISCCP database has eight updates from geostationary satellites. Conversely, the RTNEPH has some advantages over ISCCP. First, it archives data at higher horizontal resolution (48 km). Second, the RTNEPH uses conventional as well as satellite-derived observations. Last, the RTNEPH data are available in real time to selected users.

Archived nephanalysis data from the RTNEPH and 3DNEPH are available to civilian and military users (Zamiska 1986). Data are available back to 1973, with 3DNEPH-derived data covering the period prior to 1983, and RTNEPH data since. Southern Hemisphere data have been available only since 1977. AFGWC also ships the data daily to NOAA/NESDIS, the National Environmental Satellite Data Information Service, in Washington, D.C., and NRL, the Naval Research Laboratory, in Monterey, California. NMC will soon have near–real-time access to RTNEPH data through NOAA/NESDIS.

The purpose of this paper is to inform potential RTNEPH users of this unique dataset, to describe the model physics, and to document model improvements made in the last few years. Though nephanalyses have been produced at AFGWC for over 20 years, this paper is the first description available in the refereed literature. With increasing usage of RTNEPH data by the civilian community and with an increased appreciation of the importance of clouds in climate studies, we hope this paper can stimulate interest in this important field. The paper will largely consist of a description of the algorithms currently used to generate the RTNEPH; it updates technical notes on cloud analysis at AFGWC (Kiess and Cox 1988; Fye 1978), generally available only within the Department of Defense. Section 2 describes the design philosophy of the RTNEPH; section 3 describes the major components of the RTNEPH in detail; section 4 describes the limitations of the current model; section 5 indicates how AFGWC plans to address these limitations with software enhancements; and section 6 concludes with more information on how users can obtain RTNEPH cloud data.

2. Design of the RTNEPH

During the late 1970s, the U.S. Air Force decided that maintaining the poorly documented, unstructured 3DNEPH code was not worth the effort and that a total rewrite was needed. A new, structured RTNEPH code was written and implemented that allows for graceful additions of new algorithms and is easier to maintain. Like 3DNEPH, the RTNEPH synthesizes visible and infrared imagery and conventional data sources into a coherent database useful for a variety of applications. In the future, new data sources can be included with a minimum of redesign. The chosen map projection and grid structure has remained the same (Fig. 1). As shown, the RTNEPH database is on a polar-stereographic projection true at 60°N and S, and is broken up into 64 "neph boxes" per hemisphere. Within each neph box is an array of 64 × 64 analysis points.

a. Design philosophy

RTNEPH designers kept four principles in mind: speed, universality, modularity, and maximizing the probability of cloud detection.

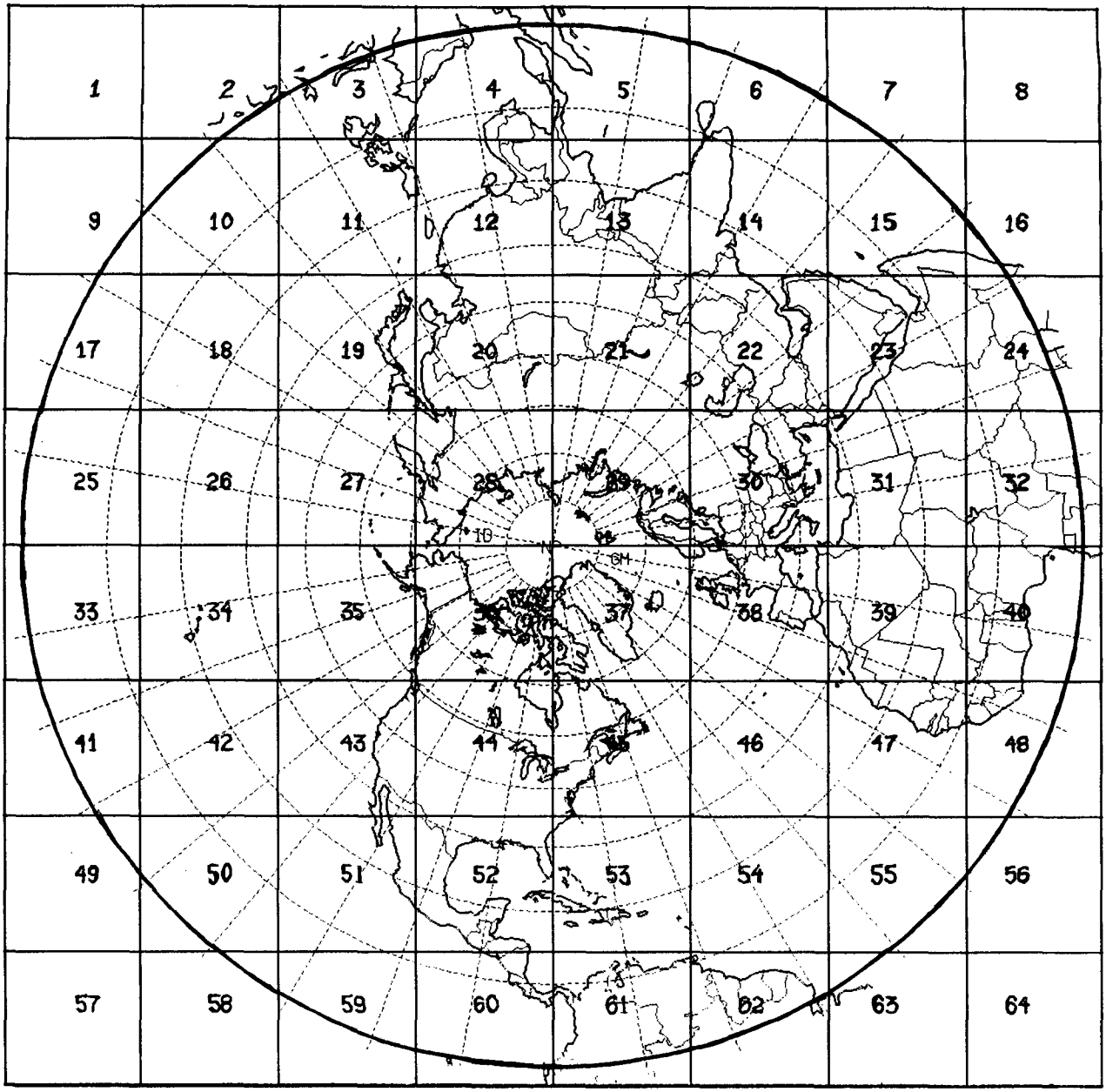

FIG. 1. The map projection for the Northern Hemispheric database. The RTNEPH grid is a polar-stereographic projection with 48-km resolution, true at 60° latitude. The projection is divided into 64 "neph boxes" as numbered, and within each box is an array of 64 × 64 analysis points. Data are stored only into the on-hemisphere analysis points.

First, because the RTNEPH is used to initialize forecast models whose output is needed promptly, it must run quickly. Currently, the RTNEPH runs on a Unisys 1100/91 mainframe computer, rated at 2.75 MIPS (million instructions per second), with 16 megabytes of memory and 3.2 gigabytes of hard-disk space. Many other satellite processing tasks (e.g., the gridding of microwave imager and sounder data) run concurrently, so the RTNEPH has simple, efficient algorithms. Many computationally expensive options such as the processing of higher-resolution imagery are being postponed because of these constraints.

Universality requires that the design must work acceptably under all circumstances of data availability. For this reason, the RTNEPH initially processes visible (VIS) and infrared (IR) imagery separately. With this method, the algorithm is not dependent on the availability of VIS data, and the RTNEPH can produce nighttime cloud analyses from IR data alone. There are other one-channel nephanalysis algorithms, the

most well known being the spatial coherence technique (Coakley and Bretherton 1982). However, AFGWC decided not to used this technique; it works properly only over radiometrically homogeneous backgrounds such as water, it requires a larger sample of satellite data than is available for the 48-km analysis point, and it is not compatible with the limited grayshade range and pixel-replication algorithm used in remapping raw imagery to AFGWC's polar-stereographic satellite imagery database.

Modularity is a software design concept that makes future modification simpler and code easier to understand. Each processor has a dedicated task. The RTNEPH has six major programs, or "processors," and a number of smaller ones. The major processors and their functions are listed in Table 1.

Last, because the air force is interested in noting any particular obstructions to vision, the RTNEPH is designed to maximize the probability of detecting cloud. If multiple sources of data are available to the RTNEPH, such as both conventional and satellite data, the RTNEPH will use the cloudiest one, provided other timeliness and proximity criteria are met.

b. Processing and data flow

The RTNEPH processes satellite data in two modes: the limited-area mode, processing only areas covered by new polar-orbiting satellite imagery, and the synoptic mode, run over all points worldwide every 3 h. The overall data and processing flow for the major processors is summarized in Fig. 2.

In the limited-area mode of processing, upon receipt of satellite data, the first step is the mapping of new data to a satellite database, called the Satellite Global Database (SGDB), which archives the data at approximately 6-km resolution. Next, the new satellite imagery data are pulled out of this database and processed by the satellite data processor into a 48-km–resolution polar-stereographic satellite analysis. Third, the merge processor then combines this satellite analysis with the surface data analysis available each hour through the conventional data processor. The synthesized nephanalysis is stored in the RTNEPH database. Operational forecasters quality control the new nephanalysis database, and the bogus processor assimilates the forecasters' changes back into the final nephanalysis. Upon completion, a short-term cloud forecast is generated over the same area. This computationally efficient trajectory-based model (Crum 1987) produces forecasts for the next 9 h to support near-term operations.

The other mode of processing is the synoptic mode, run every 3 h over both hemispheres, 1.5 h after "data time" (e.g., 1330 UTC for the 1200 UTC data time). The main purpose of this time delay is to assimilate as many new conventional cloud observations into the nephanalysis as possible so the database accurately describes the cloud conditions at one time. This synoptic RTNEPH is then used to initialize the hemispheric

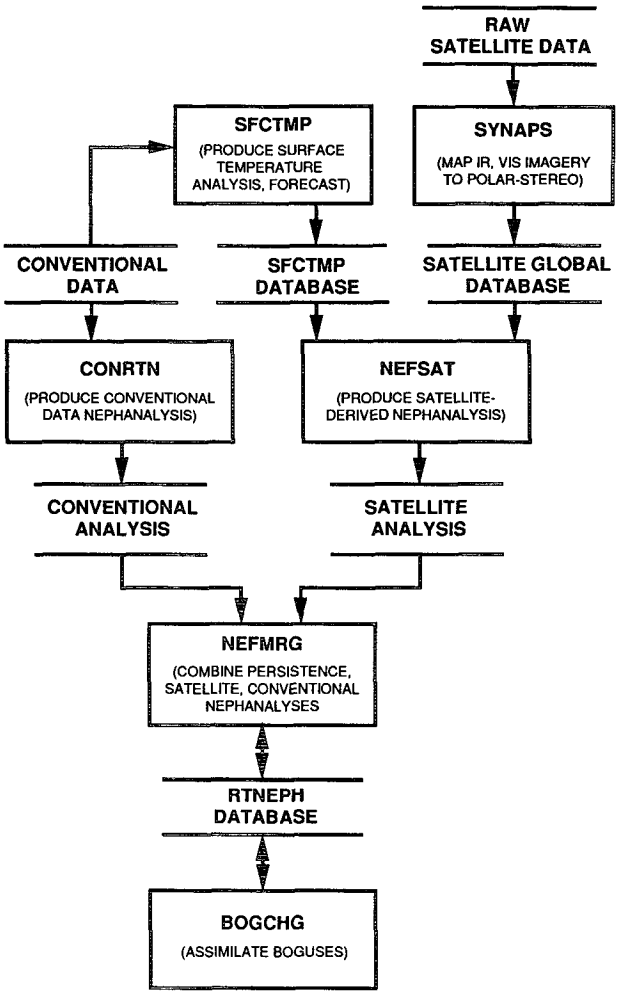

FIG. 2. Data-processing flow for the major processors (programs) in the RTNEPH. Boxes indicate the processors, and parallel lines the data stores.

TABLE 1. A list of the major RTNEPH processors and their individual functions.

Program	Function
SYNAPS	Reformats polar-orbiting satellite data into a 6-km resolution, 63-grayshade polar-stereo database.
SFCTMP	Produces a skin and shelter temperature analysis and forecast for use by NEFSAT.
NEFSAT	Produces a nephanalysis from the satellite data mapped by SYNAPS.
CONRTN	Produces a nephanalysis from the conventional (surface) observations available at AFGWC.
NEFMRG	Merges the persisted nephanalysis together with the new satellite- and conventionally derived nephanalyses to produce the RTNEPH analysis.
BOGCHG	Assimilates forecaster modifications into the RTNEPH analysis.

cloud forecast models and is also shipped to outside users (e.g., NOAA/NESDIS). In the synoptic mode, the satellite data processor analyzes any satellite data yet unprocessed. Next, the merge processor again combines the satellite and new surface data. *This output is not quality controlled.*

Many peripheral RTNEPH programs have their own processing cycles. A new 48-km–resolution global surface temperature analysis and forecast is produced every 3 h. Temperature data are used in the IR cloud detection analysis to characterize the clear scene background. Conventional cloud observations are processed into the conventional analysis database each hour. A new 381-km–resolution global upper-air analysis of temperature, geopotential height, and specific humidity is produced once each 6 h and used to determine IR-derived cloud heights. New Special Sensor Microwave/Imager (SSM/I) observations are remapped to the 48-km database as soon as the data are received at AFGWC, where they are used to enhance the accuracy of ground-temperature estimates when processing the IR imagery.

3. Detailed description of the RTNEPH processors

This section describes the six main RTNEPH processors. Each processor has a well-defined role in completing the cloud analysis. Input and output data spans a wide range of grid sizes; Table 2 summarizes the grid sizes of the nephanalysis database and some of its inputs. Henceforth, we will refer to the grid sizes according to AFGWC convention; in this system, the AFGWC's primitive equation forecast model grid (381 km) is designated "whole mesh" (Hoke et al. 1981). There are 8 × 8 whole mesh boxes within each of the 64 neph boxes on a hemisphere (Fig. 1). An array of 8 × 8 eighth-mesh boxes (48 km) fit into each whole mesh grid box, thus yielding 64 × 64 per neph box; eighth mesh is the standard resolution of the RTNEPH database and its intermediate databases. The satellite imagery database is 64th mesh (6 km).

TABLE 2. Resolutions of the RTNEPH grid structure, along with examples of RTNEPH databases that have resolutions at each grid size.

Grid size	Nominal resolution in km (true at 60°N)	Data at this resolution
RTNEPH box	3048	Archival of cloud analysis
Whole mesh	381	Upper-air temperature, height, humidity
Quarter mesh	95.25	Satellite times, viewing angles
Eighth mesh	47.625	Cloud-cover analysis, terrain heights, geography, background brightness, SSM/I microwave imagery
64th mesh	5.953	IR and VIS data

a. Satellite data mapper (SYNAPS)

Since the RTNEPH is produced on a polar-stereographic projection, AFGWC maps incoming VIS and IR satellite imagery to a database in the same projection. The processor that performs this mapping is called SYNAPS and the output database is called the satellite global database (SGDB). The SGDB consists of two hemispheric files containing 64th-mesh data. Associated control information (e.g., zenith angles, scan angles, satellite identifiers, observation times) are stored in the same files, but only for each quarter-mesh (95-km) box.

As AFGWC receives imagery from a new satellite pass each 101 min (a pass is a complete revolution of the earth by a polar-orbiting satellite), computer hardware averages the original high-resolution 3-km data to 6 km, decreasing the necessary disk storage by a factor of 4. At the same time, the temperature and albedo measurements are degraded to allow more compact storage of information; the original 256 grayshades are degraded to 63. For IR data, these 63 grayshades are a linear quantization of brightness temperature that span a range from 192 to 310 K with a separation of 1.9 K between adjacent grayshades. The hardware also cuts the pass into four pole-to-equator "quarter orbits" and sends the compacted imagery for each quarter orbit in succession to the UNISYS mainframe. SYNAPS earth-locates each imagery pixel to the proper coordinate in the SGDB, and replicates existing pixels to fill any remaining gaps between pixels on the polar-stereographic grid.

Pixel replication is done since a given 64th-mesh box on the polar-stereographic projection actually varies in size from over 6 km at the pole to near 3 km at the equator. Information from the satellite is available after the initial averaging at approximately 6-km resolution, so a one-to-one mapping of raw satellite data to the contorted polar-stereographic database can not be achieved for all points; gaps are assured in lower latitudes, and pixel duplication is required to fill each available grid box. Similarly, some of the original data is lost near the poles, as more original 6-km pixels are available than can be put into the 64th-mesh projection. Figure 3 illustrates this under- and oversampling problem.

For regions outside the viewing range of the current DMSP pass, the original, older satellite data is persisted. Thus, the SGDB is a mosaic of satellite data with different times, from near current to 6 h or more old. Figure 4 illustrates this mosaic appearance, showing the pass boundaries evident in the IR data for neph box 45 for 1550 UTC 27 August 1991.

b. Surface temperature analysis and forecast processor (SFCTMP)

Since the RTNEPH requires a high-quality, IR-derived nephanalysis, an accurate specification of the

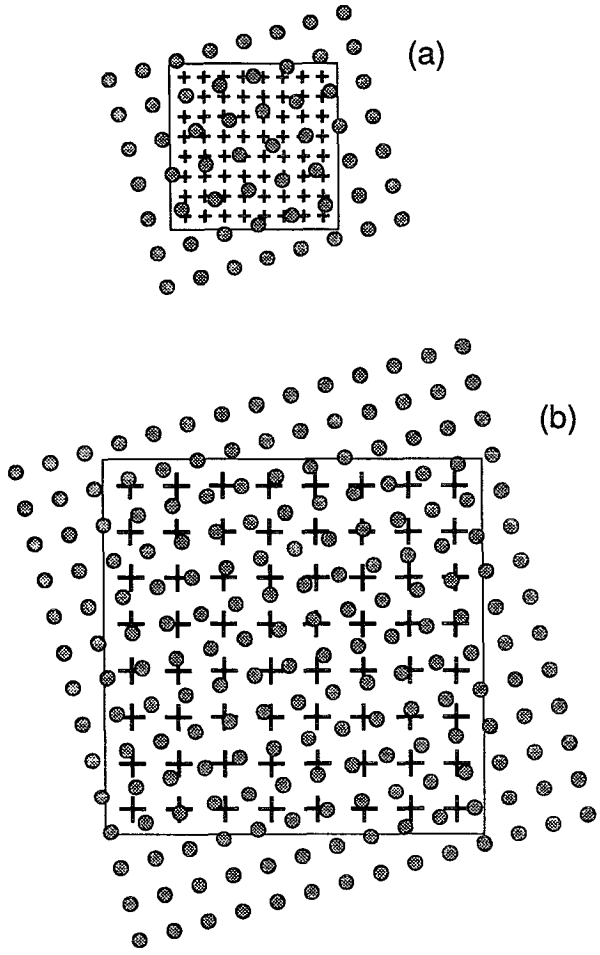

FIG. 3. Illustration of the over- and undersampling of satellite information that occurs when DMSP imagery is mapped to the polar-stereographic projection, with varying resolution. For each 64th-mesh point on the polar-stereographic projection (marked by a "+"), the nearest DMSP imagery (darkened circles) is selected. At low latitudes, the smaller grid spacing results in oversampling, or the use of original pixels more than once (Fig. 3a). At high latitudes, the large grid spacing results in undersampling, or the discarding of some original data (Fig. 3b).

surface temperature is necessary. This surface temperature is used to determine the cloud/no-cloud threshold, as will be discussed in section 3c, on the satellite data processor.

To accurately specify a background scene temperature for the IR cloud analysis, AFGWC has a global, eighth-mesh shelter and skin (i.e., ground) temperature analysis and forecast model (SFCTMP). This model runs every 3 h and produces an analysis, a 3-h forecast, and a 4½-h forecast. Forecasts are necessary because of delays in receiving surface observations worldwide. DMSP satellites are in sun-synchronous orbits, configured to overfly areas at times when surface temperatures are changing rapidly (e.g., DMSP satellite F9 flies over during midmorning), so simply using a persisted analysis would result in systematic biases of IR-derived cloud amount. By using a short-term temperature forecast instead, such biases are minimized. SFCTMP runs approximately 1 h 40 min after synoptic data time (for example, 1340 UTC for the 1200 UTC cycle) in the Northern Hemisphere, and 2 h 30 min after for the Southern Hemisphere. A large fraction of the possible surface data observations are available by these times.

On 27 April 1991, the version of SFCTMP that has been operating unchanged since 1979 was replaced with a totally new SFCTMP. For water points, analysis and forecast temperatures are derived from a U.S. Navy–supplied sea surface temperature analysis, updated daily. For land and coastal areas, the new model produces shelter and skin temperature analyses using a simplified optimum interpolation technique (Schlatter 1975). It also uses a new temperature forecast scheme based on a simplified version of the Oregon State University soil hydrology and planetary boundary-layer model (Mahrt and Pan 1984; Ek and Mahrt 1989). Whereas the older version of the SFCTMP model produced only a 3-h shelter temperature forecast, the new model extends both shelter and skin forecasts out to 4½ h, allowing near-complete temporal coverage from one cycle to the next; for example, the 1200 UTC analysis and forecast cycle produces forecasts through 1630 UTC, and the 1500 UTC analysis and forecast cycle will normally be completed around 1640 UTC.

c. Satellite data processor (NEFSAT)

NEFSAT is the satellite cloud-detection algorithm. It provides separate analyses of both VIS and IR data.

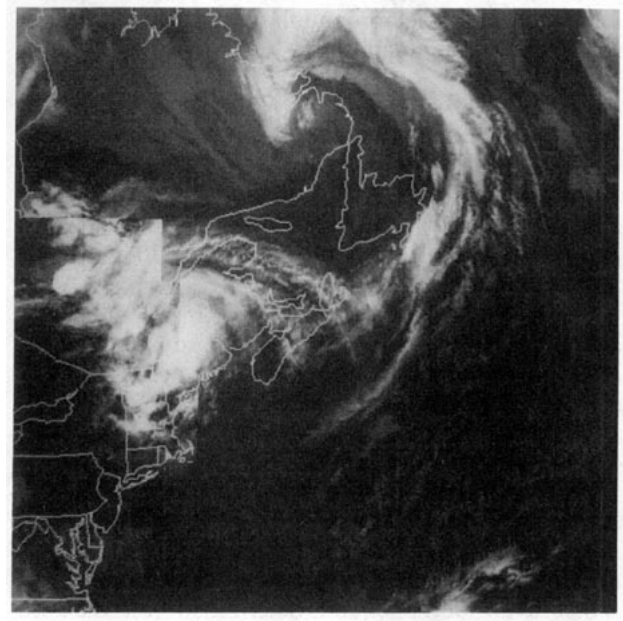

FIG. 4. Infrared image for neph box 45 at 1550 UTC 27 August 1991. Bright tones denote low brightness temperatures; dark tones denote high temperatures.

Its processing algorithm simulates the simplest algorithm a forecaster would use to analyze data. In general, the colder (IR data) or brighter (VIS data) an SGDB pixel is, the more likely it is to be cloudy. NEFSAT's algorithm makes a simplifying assumption that any pixels colder (for IR) or brighter (for VIS) than a computed clear-scene threshold are considered totally cloudy. Fractional cloud cover is derived by summing the cloudy and clear decisions for all 64th-mesh pixels within an eighth-mesh box.

NEFSAT generates separate eighth-mesh IR- and VIS-derived cloud analyses from new data in the SGDB. By separating the IR and VIS processing, nighttime or low-light processing can proceed by analyzing only the IR data. When both algorithms can be run, VIS- and IR-derived nephanalyses may determine different cloud amounts. Dealing with such discrepancies is postponed until later in the analysis scheme when the merge processor is run, where the conventional data are also assimilated.

Two nonsatellite supporting databases required for the processing of IR data are surface temperatures and upper-air temperature/humidity/height profiles. Surface temperatures are necessary to accurately estimate the satellite-sensed ground temperature used in calculating an IR threshold. For most regions, the surface temperatures are simply extracted from the database created by the SFCTMP model (see section 3b). However, for many land areas, NEFSAT also obtains an independent estimate of a satellite-sensed ground temperature from SSM/I microwave data. Upper-air temperature and height profiles are used to assign cloud-top altitudes. Humidity and temperature profiles are used to estimate water vapor attenuation, another necessary step in the determination of an accurate satellite-sensed ground temperature.

1) Infrared satellite data processing

The infrared satellite processor generates a cloud analysis from IR data in the SGDB. The IR spectral bands range from 10.2 to 12.8 μm for DMSP data, and 10.3–11.3 μm for NOAA/AVHRR (Advanced Very High Resolution Radiometer) data. Infrared satellite data is the primary and most reliable source of global cloud observations for the RTNEPH because of the frequent updates (at least four times daily) and availability of the data both day and night. The IR processor determines cloud amount by comparing measured IR brightness temperatures against an expected underlying surface temperature. If a pixel's brightness temperature is sufficiently colder than an independently derived estimate of the satellite-sensed ground temperature, cloud is detected. Cloud fraction is determined from the ratio of cloudy pixels to the total number of pixels within an eighth-mesh box. Once cloud amount has been determined, NEFSAT will also perform a layer analysis on the cloudy pixels and determine the resultant cloud type. These steps are outlined in the following sections.

(i) *IR total cloud amount*

Consider an 8 × 8 array comprised of clear and cloudy pixels, each represented by some grayshade G. The selection of a cloud/no-cloud cutoff that separates the clear and the cloudy grayshades is first made by determining the measured brightness temperature $T_{obs}(G)$ of the scene using a lookup table to convert grayshade to temperature. Then $T_{obs}(G)$ and the underlying T_{clr} are compared, where T_{clr} is an estimate of the temperature that the satellite would measure if the scene were cloud-free.

In an ideal situation, if the difference

$$\Delta T_{obs} = T_{obs}(G) - T_{clr} \qquad (1)$$

is less than zero, the pixel represented by $T_{obs}(G)$ is cloudy, since the scene being viewed has a lower temperature than the underlying surface (this assumes that atmospheric temperature monotonically decreases with height). If ΔT_{obs} is greater than or equal to 0, the pixel is warmer than the surface and thus the scene is clear.

The simple cloud/no-cloud decision in Eq. (1) is complicated by the existence of surface inversions, uncertainties in RTNEPH surface temperatures, atmospheric water vapor attenuation in IR temperature measurements, and the differing responses of individual IR sensors. With a one-channel IR threshold algorithm, there is little that can be done to detect cloud in the presence of inversions. The failure to detect the "black stratus" clouds, which appear darker than surrounding clear regions, is a recognized defect of the algorithm. However, the other problems can be addressed. For example, the amount of water vapor attenuation can be estimated. It is known that a cool, dry atmosphere will attenuate little of the upwelling surface radiation, while a warm, moist atmosphere may attenuate 10 K or more. With a knowledge of the temperature and moisture profiles, the amount of attenuation can be estimated as follows.

The RTNEPH optimizes an IR threshold calculation in two ways. First, data are adjusted to yield the most accurate possible T_{clr} (i.e., to correct for satellite or surface temperature biases and for water vapor attenuation). Two correction options have been used. Through April 1991, tables of corrections to the SFCTMP-supplied shelter temperature estimate were used. The tables were a function of: 1) satellite sensor, to account for differences in sensor response; 2) estimated surface temperature, to grossly account for the dependence of water vapor attenuation on absolute temperature; and 3) satellite scan angle and earth location, since water vapor attenuation exhibits a dependence on scan angle and latitude. No functions were available to tailor the amount of correction to analyzed air temperature and/or humidity profiles.

The new corrections, used since April 1991, take the form of a set of regression equations. Separate regression equations are used for each satellite, and for each satellite there are separate equations for day and night, and for three surface characteristics: water, land, and snow/ice. Each regression equation is of the form:

$$T_{\text{c-clr}} = T_{\text{shel}} * R_1 + T_{\text{skin}} * R_2 + (T_{\text{shel}} - T_{850}) * R_3 + P_{\text{wat}} * R_4 + \text{BBGS} * R_5 + C. \quad (2)$$

Here, $T_{\text{c-clr}}$ is the conventionally derived estimate of the IR clear-column temperature; T_{shel} and T_{skin} are the SFCTMP-supplied estimate of shelter and skin temperature, respectively; $(T_{\text{shel}} - T_{850})$ is a measure of low-level stability, with T_{850} being the 850-mb temperature derived from a global temperature analysis. This term can account for the tendency toward greater water vapor attenuation in a warm, less stable atmosphere. The variable P_{wat} refers to the precipitable water amount (in millimeters) along the scan path of the sensor, accounting for higher water vapor attenuation with greater water loading and/or at higher viewing angles. BBGS represents the RTNEPH background brightness—a general tendency toward dryness and greater swings of stability are expected for bright areas. The calculation of BBGS will be discussed later. We use R_1 through R_5 and C to represent regression coefficients and a constant, respectively, derived through regression of historical data against IR temperatures derived from a manually selected set of clear points. This new technique represents a step toward more fully utilizing the available meteorological information while remaining computationally efficient. Another advantage of the new regression equations is built-in weighting according to information content. Analysis of the weights generally showed that T_{shel} and $(T_{\text{shel}} - T_{850})$ were both reliable, whereas the other independent variables exhibited less reliability. Earlier tests with a more computationally intensive correction algorithm (d'Entremont et al. 1989; Weinreb and Hill 1980) exhibited great sensitivity to the analyzed water vapor loading; the water vapor amount was regarded as truth, so large errors in water vapor amount yielded large errors in the calculated $T_{\text{c-clr}}$. The regression method avoids this oversensitivity to errors in the input data.

Clear-column brightness temperature estimates are also available from the SSM/I sensor where its surface-type classifier (Heinrichs et al. 1990) indicates vegetated land or arable soil, deserts, or snow. These surfaces have emissivities of 0.8 to 1.0 in the SSM/I channels. Specifically, a clear-column brightness temperature estimate T_{ssmi} is derived from a linear combination of SSM/I channel brightness temperatures. The regression coefficients, which vary with surface type and satellite, were derived from historical coincident OLS IR and SSM/I temperatures of clear scenes, with the SSM/I temperatures used to estimate the IR temperature. In cloudy scenes, observed IR temperatures are significantly colder than SSM/I-estimated temperatures, since the IR channel is much more sensitive to clouds.

The final estimate of T_{clr} is derived from combining $T_{\text{c-clr}}$ and T_{ssmi} using

$$T_{\text{clr}} = W * T_{\text{c-clr}} + (1 - W) * T_{\text{ssmi}}, \quad (3)$$

where W is a weighting factor based on data availability ($W = 1$ when T_{ssmi} is unavailable), and accuracy of each estimate (generally, both are similar in accuracy, so weights are usually set at 0.5).

The second approach to optimizing the IR threshold calculation is to deal with uncertainties in the estimate of T_{clr} and to recognize the general dependence of cloud height on low-level humidity. Infrared pixels are forced to be colder than T_{clr} by an arbitrary amount before cloud is detected. This amount varies with scene background brightness, so for dark, forested regions the threshold is only a few K, while over deserts the threshold approaches 10 K. By forcing pixels to be colder than the estimate of T_{clr}, some error is allowed, and, by associating it with a surface brightness, the general dependence of cloud height on low-level moisture is implicitly recognized. For brighter areas (desert), the moisture content is lower, and clouds should have higher lifted condensation levels. Conversely, for darker backgrounds, lifted condensation levels are generally lower. Thus, the determination is made as to whether the pixel is cloudy or clear by comparing ΔT_{obs} from (1) against a predetermined term that depends on background brightness, denoted by ΔT_{clr}. Pixel fractional cloud amount $A(i)$ is then

$$A(i) = 1 \quad \text{if} \quad \Delta T_{\text{obs}} < -\Delta T_{\text{clr}},$$
$$= 0 \quad \text{if} \quad \Delta T_{\text{obs}} \geq -\Delta T_{\text{clr}}. \quad (4)$$

With each individual pixel in an eighth-mesh box now classified cloudy or clear, we can define total cloud fraction ρ_{ir} (in percent) for the analysis point as the ratio of cloudy pixels to total pixels (64); i.e.,

$$\rho_{\text{ir}} = 100 * N_{\text{cldy}}/64, \quad (5)$$

where N_{cldy} is

$$N_{\text{cldy}} = \sum_{i=1}^{64} A(i). \quad (6)$$

(ii) *Determination of cloud layers*

Having screened out the cloudy pixels, the remaining clear pixels are excluded from any further cloud processing. The cloudy pixels are then analyzed for cloud layers. From the original array of IR data, a grayshade histogram is constructed using only the cloudy grayshades. Histograms typically show peaks and valleys that in theory separate one cloud layer from the next. The job of the layer algorithm is to objectively determine where the layer grayshade boundaries are, and to pass this information on to the part of the IR pro-

cessor that determines layer cloud-top heights and amounts. The RTNEPH uses a layer-analysis algorithm that processes IR data from a 2 × 2 square of four adjacent eighth-mesh boxes. This gives a possible array of 16 × 16 pixels (8 × 8 for each box). By combining four together, some peaks and valleys in the histogram that may occur due to small sample size are avoided. A necessary result, however, is that layer grayshade boundaries are identical for all four eighth-mesh boxes.

The layering algorithm is described in more detail by d'Entremont et al. (1982) and Hawkins (1980).

(iii) *Determination of cloud amounts and heights*

Once layer grayshade boundaries are specified for each eighth-mesh box, the cloud amount for that layer is computed by counting the number of pixels with grayshade values that fall between the given layer grayshade boundaries, and dividing that count by the total number of pixels within the analysis array. In order to compute the layer-top height, the lowest IR brightness temperature for the layer is determined; the lowest temperature is presumed to be the least contaminated by upwelling background radiation and thus most representative of the true cloud-top temperature. This temperature is then corrected for atmospheric attenuation and satellite sensor biases before it is used to calculate a cloud height using a temperature–height profile valid for the location being analyzed.

Figure 4 is a picture of Northern Hemisphere neph box 45 showing the IR data from the SGDB. Figure 5 illustrates one of the end products: the IR total cloud analysis derived from the SGDB. Individual pixels determined to be cloudy have been brightened. Note in this picture that the derived product, the eighth-mesh cloud analysis, has been converted back to a higher-resolution 64th-mesh analysis for purpose of display.

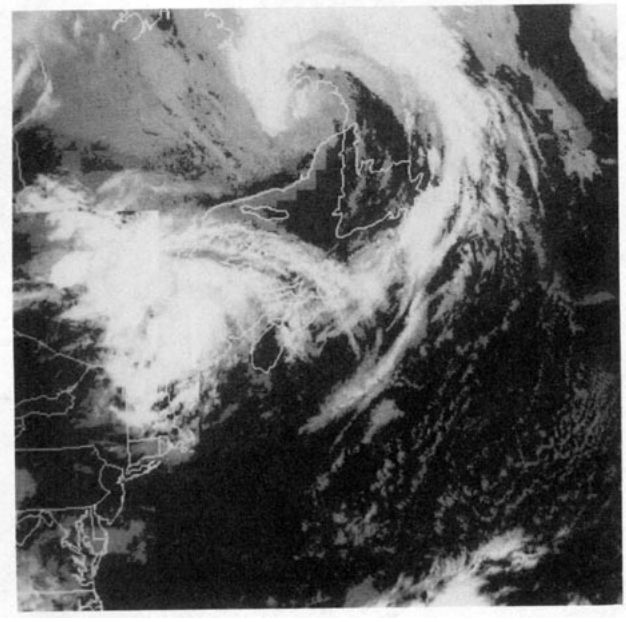

FIG. 5. Enhanced cloud analysis image for neph box 45 at 1550 UTC 27 August 1991, the same data as shown in Fig. 4. Pixels determined to be cloudy have brightness enhanced from the tones in Fig. 4.

2) VISIBLE SATELLITE DATA PROCESSING

The visible satellite data processor generates a total cloud analysis that is derived from DMSP VIS data (approximately 0.4–1.1-μm spectral bandwidth) and a database of earth surface brightness. It is essentially a threshold technique whereby satellite brightness measurements are compared to expected background brightnesses. Background brightness is the expected clear-column grayshade value as previously measured by the visible sensor. Measurements that are brighter than the background (plus an uncertainty factor) indicate the presence of cloud. Supporting databases are snow- and ice-cover analyses, and a background brightness analysis at eighth-mesh resolution. The visible processor outputs eighth-mesh total cloud cover and updates the background brightness database if conditions are clear.

The visible processor performs four main functions for each eighth-mesh box: 1) screen the data for points covered by snow, ice, or sunlight; 2) perform a cloud/no-cloud decision on each pixel within the eighth-mesh box in order to determine total cloud; 3) determine total cloud; and 4) update the background brightness analysis if appropriate. Each of these steps is outlined in the following sections.

(i) *Background screening*

The first step in the processing of the visible data is to determine whether snow or ice exists within the eighth-mesh box. Snow- and ice-cover information is supplied to the nephanalysis from the AFGWC snow analysis model (Hall 1986) at eighth-mesh resolution. Geography flags from a geography database indicate whether each eighth-mesh box is composed predominantly of water, land, ice, or coastline.

If the background contains snow or ice, then the visible clear-column grayshade will be bright and hence difficult to distinguish from cloud cover (also bright). For this reason, points flagged as containing either of these two background types are eliminated from further analysis by the visible processor. Another circumstance that prevents visible data from being further processed is if the scene contains sunglint. Scenes are flagged for sunglint processing based on background type (it must be water), scene solar geometry, and satellite position. If the scene lies within a possible sunglint area, the mean and variance of the visible grayshades are computed. If the mean is high and the variance is low, enough sunglint-contaminated pixels are likely present within the eighth-mesh box so as to be confused with

patchy low clouds. In such a case, the box is precluded from further processing. On the other hand, if the variance is high, the presence of clouds is inferred and processing will continue.

(ii) *Cloud/no-cloud decision*

Before describing the cloud/no-cloud decision programmed into the visible processor, it is first necessary to define the RTNEPH background brightness field. The background brightness grayshade (BBGS) is defined as the brightest visible SGDB grayshade that a pixel within a particular eighth-mesh box is expected to have when the pixel is cloud-free. The background brightness analysis is a dynamic database that is maintained by the RTNEPH in real time. There is one database per satellite. Updates in background brightness are necessary due to changes in snow/ice cover and vegetation (week-to-week variations), seasonal variations, and other natural effects. Figure 6 contains a background brightness field for a typical summer day. In this figure, unique values are assigned to snow (a bright white), ice (a grayer white), and water (dark), while actual background brightnesses for the remaining boxes are in shades of gray. Note the bright appearance of the Saharan desert and relatively darker appearances to forested regions.

Visible grayshades in the SGDB are representative of scene brightness. Once the background type has been determined as nonsnow or non-ice, then a cloud determination is made by comparing the average of 8 × 8 SGDB brightness values to a single background brightness grayshade for the corresponding eighth-mesh box. Clouds are determined to be present within a box if

$$\mu_{\text{vis}} \geq \text{BBGS} + \text{CUT}_8, \tag{7}$$

where μ_{vis} is the analysis box mean visible grayshade, given by

$$\mu_{\text{vis}} = 1/64 \sum_{i=1}^{64} GS_i, \tag{8}$$

where GS_i is one of an 8 × 8 array of 64th-mesh visible pixels within an analysis box, BBGS is the background or clear-column visible brightness, and CUT_8 is the analysis box mean clear/cloud threshold. CUT_8 is a measure of the uncertainty in the absolute accuracy of BBGS due to effects such as varying sun angle, bidirectional reflectance effects, surface vegetation changes, and the like. Larger CUT_8 values force differences in the mean brightness and corresponding background brightness to be larger before clouds are detected. In other words, extra precaution is taken to ensure that an incorrect clear-cloud decision is not made; this generally reflects uncertainty in either the satellite measurements, the background characteristics, or both. Generally, CUT_8 values are larger over brighter scenes, reflecting the greater difficulty in distinguishing cloud over desert. BBGS is a function of satellite sensor, geographic location, and time (e.g., time of day, time of year); CUT_8 depends on BBGS and satellite sensor, and is manually updated as conditions warrant.

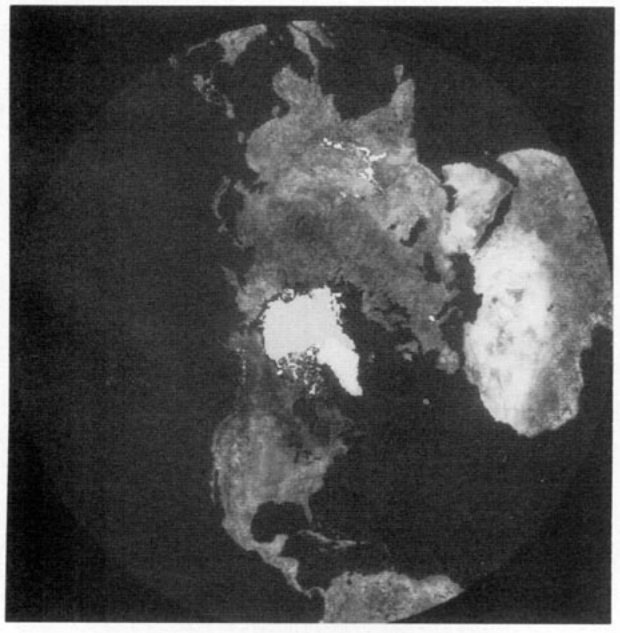

FIG. 6. Northern Hemisphere background brightness for DMSP satellite F9 at 1550 UTC 27 August 1991.

(iii) *Total cloud determination*

The cloud/no-cloud decision is made first by the visible processor on an eighth-mesh box basis as specified by Eq. (7). Once this test is passed, a more detailed cloud analysis is made on a pixel-by-pixel (64th-mesh) basis within the "cloudy" eighth-mesh box. A clear/cloud grayshade cutoff GS_{cut} is calculated for the box using

$$GS_{\text{cut}} = \text{BBGS} + \text{CUT}_{64}, \tag{9}$$

where BBGS is the background brightness and CUT_{64} is the "64th-mesh" parameter, analogous to CUT_8, that accounts for the variability of individual pixel VIS grayshade values within the eighth-mesh box. Like its eighth-mesh counterpart, CUT_{64} is a function of satellite sensor, background brightness grayshade, and time (of day, year, etc.). Once GS_{cut} is computed, the number N_{cldy} is determined; N_{cldy} is the number of 64th-mesh pixels within the analysis box that have values greater than or equal to GS_{cut}. The percent total cloud cover ρ_{vis} as computed by the visible processor is then simply

$$\rho_{\text{vis}} = 100 * N_{\text{cldy}}/64. \tag{10}$$

Values of the visible grayshade mean and variance are also computed and stored for later use by the RTNEPH

cloud-typing program. These latter statistics include both clear and cloudy pixels.

An example of visible satellite data is shown in Fig. 7, and an example of the corresponding visible nephanalysis is depicted in Fig. 8. Again, pixels brightened from Fig. 7 represent cloudy regions as determined by the nephanalysis.

(iv) *Background brightness update*

The background brightness field is a dynamic database that is monitored and updated by the RTNEPH in real time. It is updated automatically as a by-product of the cloud analysis. There is one database for each satellite. Kiess and Cox (1988) summarize the tests a point must pass before updating is allowed. In general, the RTNEPH is conservative in updating the background brightness field to ensure no contamination by cloud, snow, or sunglint.

3) CLOUD TYPING

The output from the satellite data processor includes a distinct cloud type for each layer detected by the IR processor. Cloud typing will depend upon the IR-derived cloud height, the variance of IR pixel grayshades in a cloud layer, the mean IR brightness temperature, and, if available, the variance of the 64 visible pixels within the analysis point.

The first step in this process is to decide if the cloud is a low-, mid-, or high-level cloud. For each layer archived by the IR processor, the cloud height obtained from the layer analysis is compared to a fixed mid- and high-cloud threshold. If the aboveground layer height is 6500 m or greater, it is typed as high cloud; if greater than or equal to 3000 m but less than 6500 m, it is typed as mid cloud; if less than 3000 m, it is typed as low cloud.

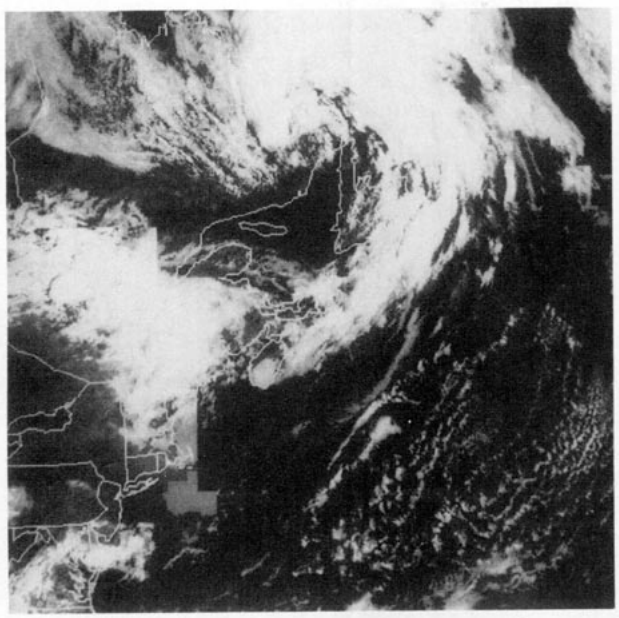

FIG. 7. Visible grayshades for neph box 45 at 1550 UTC 27 August 1991. Bright tones denote high reflectance; dark tones denote low reflectance.

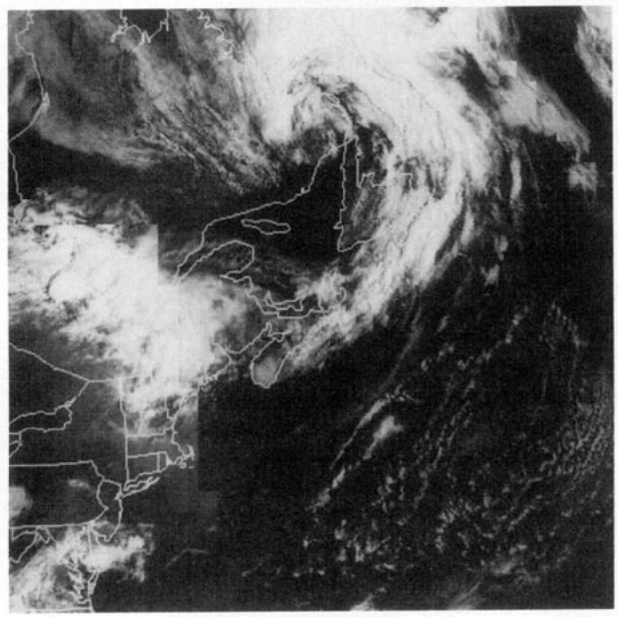

FIG. 8. Visible nephanalysis for neph box 45 at 1550 UTC 27 August 1991, the same data as in Fig. 7. Pixels determined to be cloudy have brightness enhanced from the tones in Fig. 7.

Next, the cloud-typing processor attempts to distinguish between cumuliform and stratiform clouds by examining the IR grayshade variance and, if available, the VIS grayshade variance. The underlying philosophy is simple; the greater the variance, the more cumuliform the cloud. An index is calculated for both the IR layer variance and the VIS variance. If visual data are not available, the VIS index is arbitrarily assumed stratiform.

Once the level and variance information are available, a cloud-type decision is made based on the decision matrix shown in Table 3. A final cloud type of cumulonimbus (CB) is determined when the cloud-top height is greater than 5486.0 m (18 000 ft) and the mean IR brightness temperature is less than 228 K. AFGWC recognizes that the low height threshold contributes to an overabundance of CBs and plans to raise this height in the future to a more realistic value.

d. Conventional data processor (CONRTN)

There are known deficiencies with satellite-derived nephanalyses, such as an inability to accurately detect low clouds and cloud bases using IR data. For this reason, the RTNEPH retrieves cloud parameters from conventional (surface-based) observations each hour and stores them to another eighth-mesh database so it

TABLE 3. Cloud types as specified by visible and IR grayshade variances, and the IR-derived cloud height.

Visible variance	Infrared variance: Cumuliform (high)	Infrared variance: Stratiform (low)
Cumuliform (high)	High: CI Mid: AC Low: CU	High: CI Mid: AC Low: SC
Stratiform (low)	High: CI Mid: AC Low: SC	High: CS Mid: AS Low: ST

High: cloud tops > 6500 m.
Mid: 3000 m < cloud tops ≤ 6500 m.
Low: cloud tops ≤ 3000 m.

can supplement the satellite-derived nephanalysis where appropriate. The program that stores these data is the conventional data processor, called CONRTN. It runs approximately one-half hour after data time (e.g., 1230 UTC for the 1200 UTC data) and uses both standard hourly and synoptic observations in the production of a nephanalysis. Kiess and Cox (1988) describe the processing algorithm in more depth.

The overall philosophy of this module is to produce one "best report" on cloud conditions for each eighth-mesh box inside which a conventional observation is available; all other boxes are left blank. This best report will contain total and layered cloud amounts, layered cloud types, bases, tops, present weather, and visibility. If any of these parameters are not available from the conventional data, they are flagged as "missing." Most eighth-mesh boxes will contain zero or one observation, but if more than one are available, a best report is selected as follows: first, all observations older than 3 h are not considered; second, the report with the highest total cloud is used, regardless of whether a more recent report has lower cloud amount. If two reports have identical total cloud, the report with the lowest cloud base is used. If cloud bases are again the same, the most recent report is used. If the report indicates low-level clouds, older reports (up to 3 h) are then searched for additional cloud information above the lower-level cloud deck. These processing rules maximize the probability of detecting any obscurations to vision, one of the RTNEPH design principles mentioned in section 2.

e. Merge processor (NEFMRG)

The merge processor has the task of assimilating conventional and satellite-derived nephanalyses into a robust, consistent database. The satellite-derived nephanalysis cannot stand on its own because it produces separate analyses for IR and VIS data, and it makes no attempt to define cloud bases. Similarly, the conventional database is unsuitable for use as a final cloud analysis because of the relatively few observations worldwide, yet it can be beneficial in defining lower cloud layers not detected in the satellite-derived cloud analysis. Thus, an intelligent merging of these data sources produces a better final cloud analysis than either would alone.

As the merge processor runs, it produces a final cloud analysis from three sources: the persisted (previous) RTNEPH cloud analysis, the satellite cloud analysis from NEFSAT, and the conventional cloud analysis from CONRTN. This final cloud analysis is produced in a series of steps executed in sequence for each analysis box considered. These steps are summarized in Fig. 9. The first step is to read in the persisted RTNEPH database. Next, conventional data are combined with the persisted nephanalysis, and finally, the new satellite data are combined and the output stored to the database. There is a complex set of rules for the data assimilation with each step. These rules have been developed over many years through extensive scrutiny of the satellite and conventional data by operational forecasters at AFGWC. These rules are explained in the following paragraphs.

1) CONVENTIONAL DATA ASSIMILATION

Before allowing the assimilation of conventional data for an eighth-mesh box, NEFMRG checks the persisted RTNEPH database to see if it has been quality controlled, or "bogused," recently. If it has been bogused *recently* (a user-definable time threshold currently set at 120 min), no new satellite or conventional data are

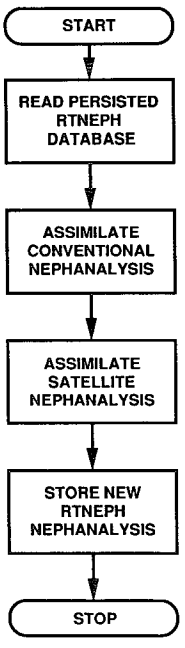

FIG. 9. High-level design of the RTNEPH merge processor.

allowed to overwrite this eighth-mesh box. Since the box has been recently bogused by a forecaster, his evaluation of the cloud cover is assumed to be more realistic than a new satellite or conventionally derived nephanalysis.

For points without recent boguses, the next step is to assimilate the gridded conventional observations from CONRTN with the persisted RTNEPH into a "combined analysis." First, where available, the gridded conventional cloud nephanalysis replaces the persisted nephanalysis. After this, the merge processor "spreads" the conventional observations, taking the isolated observations and allowing their cloud information to be copied to adjacent eighth-mesh boxes, provided those boxes didn't already have conventional data. This expands the influence of conventional observations so that a higher percentage of the eighth-mesh boxes worldwide will have new hourly information. Currently, high- and mid-cloud observations are spread two boxes; low clouds, one box; and clear areas, three boxes. These spreading distances are based on estimates of how far an observer can see toward the horizon with varying cloud height. Spreading of any height cloud is limited to one eighth-mesh box along a coastline. If two conventional observations could potentially spread to a new box, the nearer of the two is chosen. If both are equally distant, the more timely of the two is chosen. If the two are equally timely, the one with the lesser cloud cover and higher visibility is chosen, since the observer at the point with less cloud probably was better able to factor in the cloud cover in that adjacent area. Finally, spreading is limited in complex terrain. If the terrain height of the grid point being spread to is greater than the cloud base, the cloud base is raised to the terrain height. If the terrain is higher than the cloud top of the conventional observation being spread, the spreading to this grid point is not performed.

The method for assimilating the new Automated Surface Observing System data has not yet been decided.

2) SATELLITE DATA ASSIMILATION

Next, the merge processor assimilates new satellite-derived nephanalysis data where available. Again, it considers only boxes that do not have a timely bogus. The first step here is to fill in missing cloud tops and bases, both for the conventional observations and the IR-derived nephanalysis, respectively. To determine these, a default thickness is added to the available base or top. The default thicknesses for acceptable RTNEPH cloud types are listed in Table 4. If no cloud-height information is supplied by the conventional data, a climatological value for low, mid, or high cloud base is assigned, and the cloud top is again calculated using default thicknesses.

The assimilation philosophy now becomes more involved; it is explained graphically by Fig. 10. For each eighth-mesh box, a decision is made concerning which cloud layers in the combined analysis to use and which to discard. This decision is based on a comparison of the timeliness of the combined analysis and the satellite analysis. If the satellite analysis is older or the same time as the combined analysis, as would happen if the DMSP satellite had not flown over the point recently and the combined analysis provided a new surface observation, then the final nephanalysis consists solely of the combined analysis.

TABLE 4. Default cloud thicknesses used by the RTNEPH merge processor.

Cloud type	Thickness (m)
Cumulonimbus	6500
Stratus	300
Stratocumulus	1800
Cumulus	2000
Altostratus	1000
Nimbostratus	1800
Altocumulus	2000
Cirrostratus	1000
Cirrocumulus	1800
Cirrus	2000

If the time for a given box in the satellite nephanalysis is only slightly newer than the combined analysis time ("slightly newer" is user definable, currently set at 70-min-or-less time difference), then the satellite analysis is preferentially weighted over the combined analysis. The general rationale is that the satellite analysis should be more reliable since it is newer, but it may not detect low cloud with its threshold method. Thus, if the satellite detects no cloud, it would be prudent to preserve a conventional observation's low cloud but any higher cloud should already be detected by satellite. However, if the satellite observation detects any cloud, its full view of the box is obstructed and all the information content of the conventional observation should be preserved. Thus the algorithm specifies that middle and high clouds will be stripped from the combined analysis if the satellite observation indicated clear conditions. Similarly, if the satellite observation was cloudy, the layer structure of the combined analysis is preserved.

Next, consider the case when conventional data are of intermediate age, i.e., the combined observation is not drastically older than the satellite observation. Again, "intermediate" is user definable; currently this refers to a combined nephanalysis time between 70 and 90 min older than the satellite-derived nephanalysis. In this case, mid and high clouds are always stripped away from the persistence nephanalysis; only the remaining low cloud needs to be assimilated with the satellite nephanalysis into the final cloud analysis. It is assumed that higher-level clouds, subjected to greater-magnitude winds aloft, are likely to advect beyond the eighth-mesh box and thus should be removed in favor of the more recent satellite input.

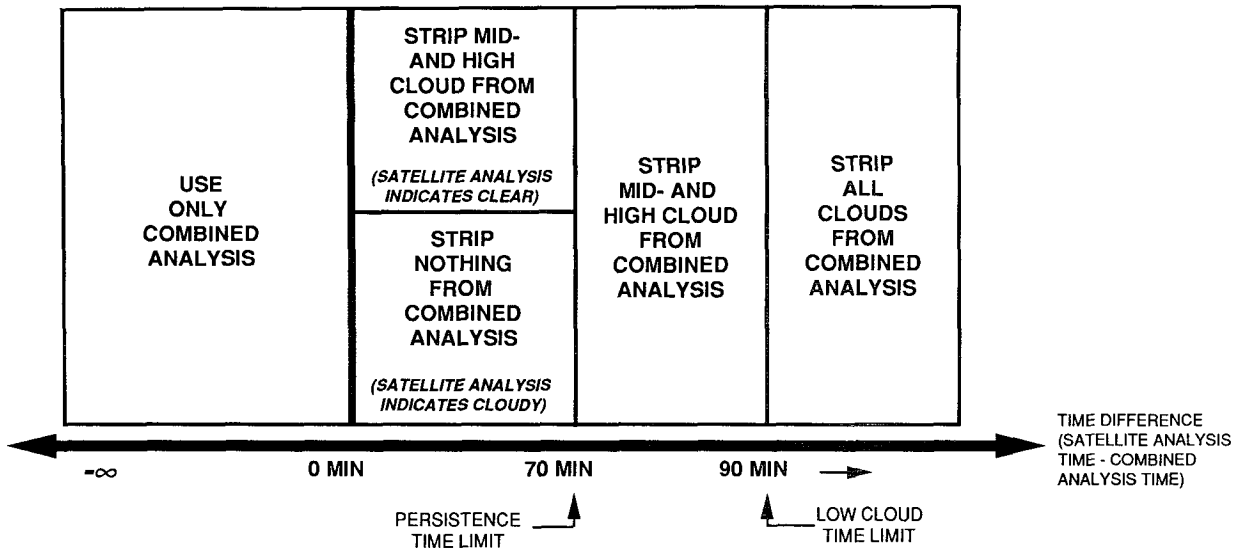

FIG. 10. Venn diagram depicting how cloud layers in the combined nephanalysis data are treated based on a comparison with the age of the satellite nephanalysis.

If the satellite analysis is much newer, satellite data totally overwrite the combined nephanalysis. The philosophy here is that beyond this time, the combined analysis is not useful. This is illustrated in the rightmost box in Fig. 10.

A few ambiguities remain, notably how satellite nephanalyses derived from VIS data are assimilated, how to account for upper-layer clouds obscuring lower-layer clouds in the satellite-derived analysis, and how cloud layers are arranged into the final database. For VIS data, an extra-low cloud layer is added to the final cloud analysis if a timely VIS-derived observation indicated more cloud than an IR observation. In such a case, a stratus cloud with a layer amount equal to the difference between the VIS and IR total cloud amounts is inserted. The stratus cloud is placed at a height of 620 m above ground level, and the default stratus thickness from Table 4 is used to calculate the cloud-top height. The rationale here is that the missed IR cloud in all likelihood is low cloud or fog because of the limitations of the IR threshold method.

If the satellite processor detected more than one cloud layer for the box, the lower layer amounts are increased to account for the percent that was obscured by the higher-level clouds. The equation determining the increase, I, is

$$I = (\mathrm{CL}*\mathrm{CA})/(100 - \mathrm{CA}), \qquad (7)$$

where CL is the current layer amount from the IR-derived satellite nephanalysis, and CA is the layered cloud amount above; I, CL, and CA are all expressed in percent. Then, I is added to CL to determine the new layer amount.

The final step of the merge processor is to sort the layers in order of decreasing height of cloud base and, if necessary, to merge layers together so no more than four layers exist for a grid point (four is all the RTNEPH database can hold). If no more than four layers exist, nothing is done. If more than four exist, then Table 5 is used to determine compatible cloud types for merging. Starting with the first layer, each other layer is searched to determine if it is compatible for merging. A "1" in Table 5 indicates that cloud types are compatible. If two layers are compatible, then the more cumuliform type is chosen, and the higher cloud-top height and lower cloud-base height are chosen for the final output. The selection of cloud-layer amount depends on from which analysis (persistence, conventional, or satellite) the layer was derived. If the two layers to be merged are both satellite derived, the final layer cloud amount is the sum of the two layer amounts. If not, the larger of the two amounts is chosen.

Figure 11 shows a color composite picture simulating an RTNEPH total cloud analysis after the merge processor. This picture is generated from the same cloud

TABLE 5. A list of compatible cloud types for merging. "1" indicates that the merging of these two types into one cloud layer is allowed.

	CB	ST	SC	CU	AS	NS	AC	CS	CC	CI
CB	1									
ST		1	1	1						
SC		1	1	1						
CU		1	1	1						
AS					1	1	1			
NS					1	1	1			
AC					1	1	1			
CS								1	1	1
CC								1	1	1
CI								1	1	1

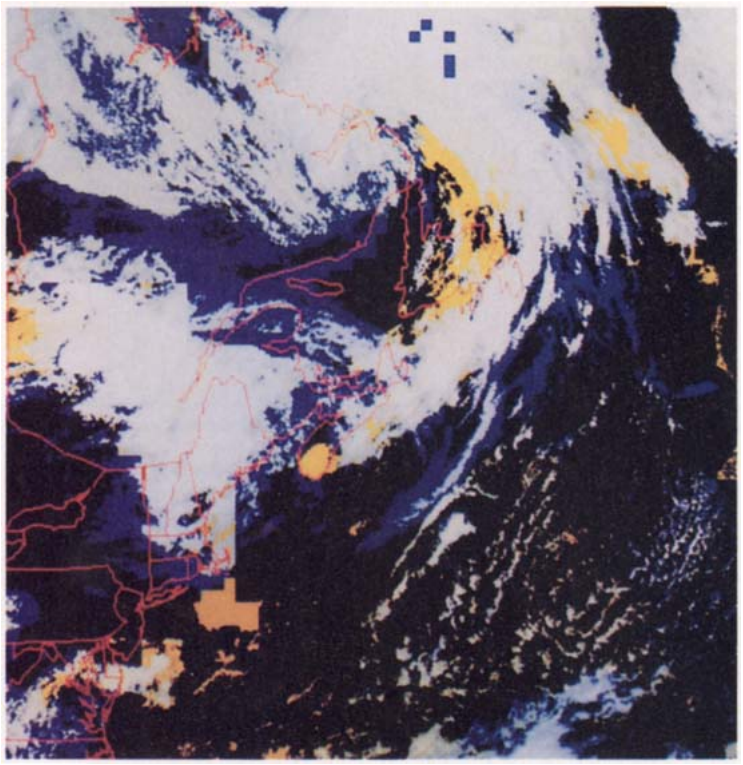

FIG. 11. A color composite of the 1550 UTC 27 August 1991 total cloud analysis synthesized by combining the IR and VIS total cloud analyses. IR-derived clouds are blue; VIS-derived clouds are yellow; IR- and VIS-derived are white; and clear areas are black.

analyses shown in Figs. 5 and 8. In this picture, the infrared and visible total cloud analyses were synthesized and reconverted from their normal eighth mesh back to 64th mesh for purposes of illustration. Clear areas are black. Pixels typed as cloudy in the final analysis by only the IR processor are colored blue; similarly, pixels typed as cloudy in the final analysis by only the VIS processor are yellow. Pixels typed as cloudy by both retain a whitish color. Note that when viewing the output of the RTNEPH merge processor, the user would normally also see some scattered areas affected by conventional cloud reports. In order to simplify the illustration, these were not included here.

f. The bogus processor (BOGCHG)

The automated algorithms for processing IR, VIS, and conventional data in the RTNEPH do not always produce a high-quality cloud analysis. For example, low clouds often are not well analyzed by NEFSAT's IR processing algorithm when the cloud-top temperature is very similar to the ground temperature. Quality control by trained forecasters is thus an important part of the RTNEPH. Immediately after a new quarter orbit of satellite data has been processed by SYNAPS, NEFSAT, and NEFMRG, displays of the RTNEPH database and the new satellite imagery are shipped to a graphics workstation. Using the workstation, trained forecasters overlay the nephanalysis cloud amounts on displays of the latest satellite imagery. They note the areas where, in their judgment, total cloud is not correctly analyzed, draw a perimeter around the area using a graphics tablet and mouse, and label points within the perimeter with a layer cloud amount and type.

Once the whole quarter orbit has been examined by a forecaster and all misanalyzed areas bounded and labeled, the bogus information is packed into a file and shipped back to the UNISYS mainframe, where BOGCHG, the bogus processor, assimilates the new changes into the RTNEPH database. Because forecasters cannot define a cloud top or base, BOGCHG must insert the boguses of amount and type and supply an internally generated cloud top and base. The cloud-top and -base heights are set from the cloud type defined in Table 6.

BOGCHG must also rearrange the cloud layers in a consistent manner, as well as recompute a total cloud. For example, within a particular area, the RTNEPH may have originally analyzed 3/8 stratus cloud and 1/8

TABLE 6. A list of the default cloud tops and bases used for bogused cloud values in the RTNEPH.

Cloud type	Base (m)	Top (m)
Cumulonimbus	915	9157
Stratus	152	458
Stratocumulus	762	1524
Cumulus	915	2134
Altostratus	2135	3353
Nimbostratus	1829	3658
Altocumulus	2439	4268
Cirrostratus	5487	8231
Cirrocumulus	6097	8536
Cirrus	6097	8536

cirrus, and the forecaster may have added a thin cirrostratus layer of 5/8 coverage. BOGCHG will redefine the RTNEPH database to have two cloud layers, a 3/8 stratus and a 5/8 cirrus, and will recompute the total cloud. The algorithm is described in further detail in Kiess and Cox (1988).

4. RTNEPH limitations and problems

Users of RTNEPH output need to be aware of its limitations. Certain things are done well in the RTNEPH; others are done poorly. This section will discuss the general accuracy of each of the stored parameters resulting from the choice of algorithms. Readers are also referred to Henderson-Sellers (1986) for a critique of the old 3DNEPH accuracy by climatic regime.

One of the most frequent misconceptions about the RTNEPH database is that it is synoptic. Indeed, a new RTNEPH database is shipped every 3 h to ETAC, but only those few points in the database with conventional cloud observations are valid at the synoptic time. The rest of the final nephanalysis is mostly satellite derived, and, therefore, rarely valid at the synoptic data time. The RTNEPH is constrained by its input satellite data, which comes from polar-orbiting satellites. These satellites pass over each point on the earth approximately twice each day (more often near the poles). This guarantees large gaps in the temporal frequency at which a given eighth-mesh box is updated, unless there are conventional data available for the box. With the 1991 constellation of two DMSP satellites, one that passes over at approximately 6:00 A.M. and P.M. LST, and the other that passes over approximately at 9:30 A.M. and P.M. LST, there are large data gaps through the late morning, afternoon, and the nighttime hours. Figure 4 illustrates the mosaic look of the input satellite data; the output RTNEPH has a corresponding mosaic.

The RTNEPH is still far from being able to produce a perfect cloud analysis even with new satellite data. AFGWC has coded the RTNEPH to concentrate foremost on cloud detection, with less emphasis on cloud height, thickness, and type determination.

a. Cloud-amount problems

The RTNEPH must rely mostly on its IR-derived nephanalysis, since conventional data coverage is sparse and VIS data is not useful either at night or by DMSPs with sun-synchronous orbits over the terminator (day/night boundary). By relying on the IR threshold method for cloud detection, the RTNEPH is vulnerable to misinterpreting low cloud amount. Many low clouds go undetected with the threshold method. This is especially true for stratus associated with lower-troposphere temperature inversions that occur at night or over snow and ice. For these "black stratus" clouds, the assumption that the cloud-top temperature is colder than the ground temperature is invalid. In such cases, cloud amounts are usually bogused to a more realistic amount by a trained forecaster.

Even when a cloud top is indeed colder than the ground temperature, the RTNEPH may misanalyze it. AFGWC's surface temperature model and water vapor attenuation scheme are not perfectly accurate, with a worldwide land rms error of approximately 3–4 K in estimating the true IR clear-column temperature. This inaccuracy causes errors in determining an appropriate cloud/no-cloud temperature threshold and an over- or underanalysis of cloud amount. Once again, most of these errors are corrected by forecasters during the quality control process.

Another serious problem of the RTNEPH database is the tendency to overanalyze clear or totally cloudy conditions and underanalyze the extent of partly cloudy scenes. This results from the SGDB's large pixel size (6 km) and the assumption that each of the 64 pixels within an eighth-mesh box is either totally clear or totally cloudy, rather than fractionally covered with cloud. For this cloudy/clear assumption to be more accurate, the pixel size in general would have to be much smaller (Wielicki and Welch 1986). The consequence of this is shown in Fig. 12, a plot of the frequency of distribution of total cloud for the IR-, VIS-, and conventionally derived nephanalyses. Both the IR- and VIS-derived analyses show a markedly stronger tendency to analyze no cloud cover or complete cloud cover than the conventional analysis. Admittedly, surface-based observations are biased toward partly cloudy analyses, but are more likely to represent an accurate frequency distribution of total cloud than the RTNEPH satellite-derived analyses.

The accuracy of layered cloud amounts is even more suspect. Unless a point is supplemented with a conventional observation, the RTNEPH has no way of detecting low- and midlevel clouds when there is an obscuring high-level cloud deck, or of assigning an accurate cloud thickness.

b. Cloud-height problems

The accuracy of cloud heights in the RTNEPH has not been extensively studied. However, it is believed

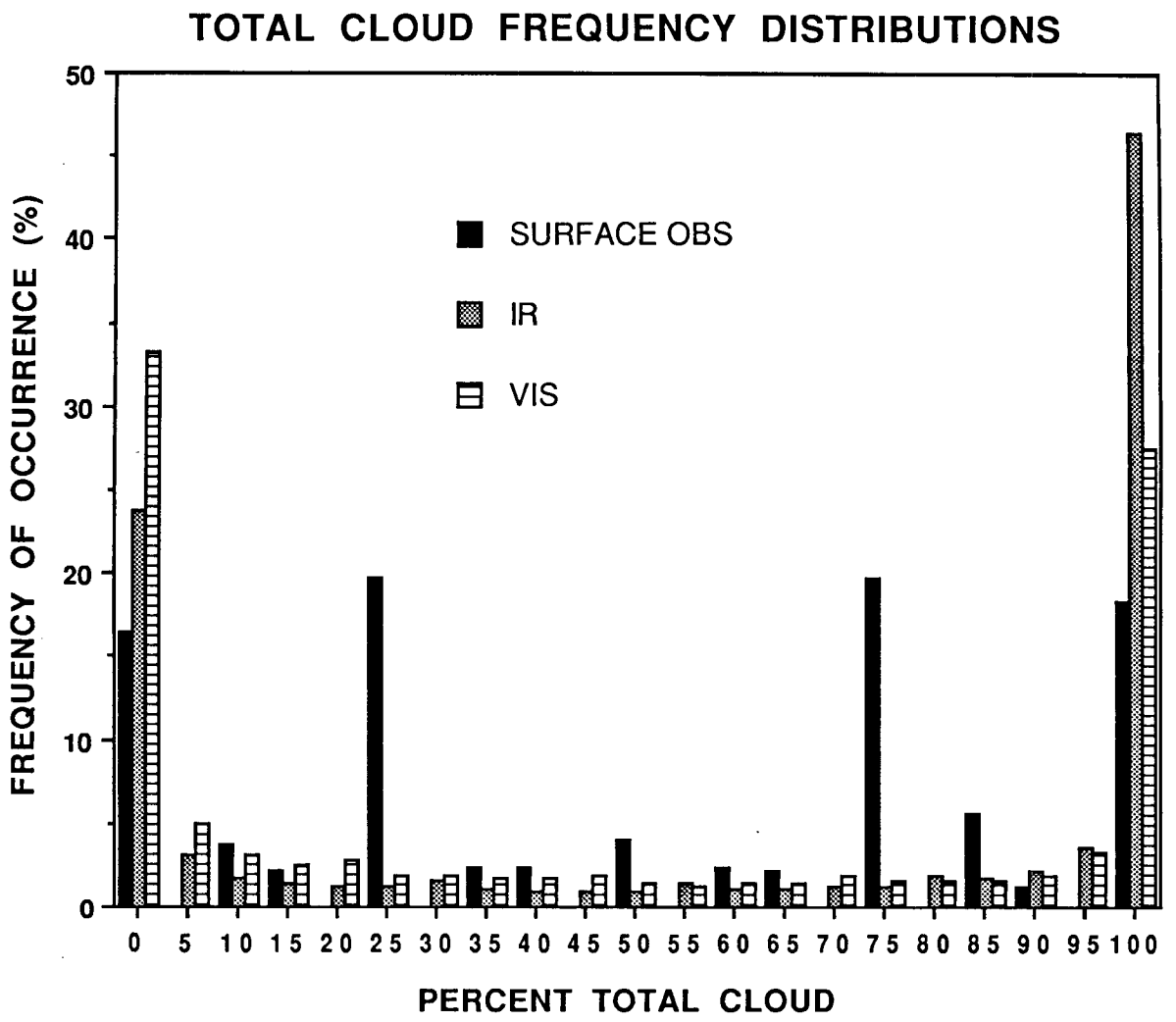

FIG. 12. A frequency distribution of Northern Hemisphere total cloud amount for 1200 UTC 28 August 1991, derived from the RTNEPH conventional analysis, the IR-derived nephanalysis, and the VIS-derived nephanalysis.

the RTNEPH both underanalyzes the frequency of thin clouds, especially cirrus, and generally places these clouds at lower-than-appropriate elevations (Henderson-Sellers 1986). Once again, this problem results from the assumption that each pixel is either totally cloudy or totally clear and that each cloudy pixel has an IR emissivity of 1.0. Thus, the RTNEPH assumes that no upwelling radiation from the surface is transmitted through the cloudy pixel, when, in truth, this frequently happens. As a result, the actual cloud temperature is often much colder than the pixel's satellite-measured brightness temperature, and yet pixel temperature is used as the representative temperature of the cloud top when determining its height.

c. Cloud-typing problems

As explained in section 2, RTNEPH cloud typing is based on two simple criteria: the cloud height, and the pixel grayshade variance within a layer cloud grayshade interval. This simple typing method does an adequate job of differentiating between cumuliform and stratiform clouds, but little else. Errors in cloud height cause cirriform and midlevel clouds to be incorrectly typed as lower clouds due to the simplifying assumption of a cloud emissivity of 1.0.

A final typing problem is an overabundance of cumulonimbus clouds. This overabundance results from a low height threshold for cumulonimbus in NEFSAT. This problem will be corrected in the near future.

5. Planned improvements

The RTNEPH, as described in section 2, was recently upgraded with a new regression scheme to estimate water vapor attenuation to produce a highly accurate clear-column IR temperature estimate. Also, the surface temperature analysis and forecast model was re-

placed. Both of these should increase the model's ability to discriminate between low clouds and the surface. AFGWC hopes to improve the RTNEPH further. The following improvements will be made, funding and manpower permitting.

a. Visible data-processing improvements

As of May 1991, the RTNEPH processed VIS data from only the daylight quarter orbits on the DMSP F9 satellite, which passed overhead at approximately 0930 LST. Follow-on DMSPs were planned to be in orbits nearer the terminator, making the use of VIS data more complicated. At the lower solar-elevation angles that would accompany these new orbits, sunglint over water will become more pronounced, as will the variation of land albedo from the eastern edge of the satellite pass to the western edge. AFGWC has a technology transition project with the U.S. Air Force's Phillips Lab (PL) Satellite Meteorology Branch to study possible improvements in processing VIS data. Under this agreement, PL develops research-grade algorithms, tests them, and then transfers the prototype code to AFGWC for implementation. The likely approach to improving VIS processing will be to perform bidirectional reflectance calculations to more precisely determine the surface clear-column albedo. Phillips Lab has not yet decided whether these calculations will be taken from previously derived *NIMBUS-7* calculations (Taylor and Stowe 1984) or rederived specifically to the DMSP VIS sensor.

Another likely improvement to VIS data processing will be the incorporation of an algorithm to correct for the dependence of cloud cover on viewing angle. Typically, the analyzed cloud amount increases with increased viewing angle (i.e., as the satellite's VIS/IR data sensor scans obliquely, rather than straight down). Phillips Lab will probably select for transfer the algorithm developed by Snow (1990) and validated by Minnis (1989). This algorithm assumes a domed, cylindrical cloud shape and permits determination of actual cloud fraction from the apparent cloud amount.

b. Improved satellite database

The RTNEPH may be significantly improved by redesigning the front-end database, the SGDB, used to archive the satellite data that feeds into NEFSAT. Currently, this database can not archive any NOAA/AVHRR multispectral data or geostationary satellite data. Further, it cannot store DMSP data at its full spatial resolution (3 km) and temperature resolution (256 grayshades, or ~0.5 K between adjacent grayshades). Redesigning this database will allow storage of both data sources at their highest resolutions. This will improve the RTNEPH by providing more data and by making the analysis truly more synoptic, thereby enhancing the nephanalysis quality. Furthermore, the smaller pixel size will reduce the errors due to subpixel-resolution clouds. This improvement must wait until AFGWC computer facilities are upgraded, however.

c. Multispectral and GOES data processing

If a new satellite database becomes available and there are sufficient computational resources, AFGWC plans to develop new algorithms to process multispectral data from the AVHRR sensor aboard NOAA polar-orbiting satellites. This AVHRR sensor supplies a wider range of available imagery [two VIS channels, one 0.55 to 0.70 μm, and one 0.72 to 1.1 μm; two IR channels, one 10.3 to 11.3 μm, and one 11.5 to 12.5 μm; and an intermediate channel (3.5 to 3.9 μm)]. Most of the techniques rely on interchannel comparisons of reflectivities or brightness temperatures. These are useful for low cloud detection, snow/cloud discrimination, cirrus detection, and the tendency for the nephanalysis to underanalyze the frequency of partly cloudy scenes—some of the most notable problems with the current RTNEPH. The most likely candidate algorithms are discussed in Saunders and Kriebel (1988), d'Entremont (1986), and Allen et al. (1990). These algorithms could also be used for the processing of DMSP multispectral data when it is available (possibly mid-to-late 1990s). Also, AFGWC has just begun to explore ways GOES-Next and other geostationary satellite information can be included.

6. Concluding remarks

The U.S. Air Force Real-Time Nephanalysis model, the RTNEPH, has been described in detail. Along with its predecessor, the 3DNEPH, it has been providing global cloud-analysis data for 20 years. These data are quite useful for numerical model initialization and verification, and also for climate studies that need cloud information for radiation feedback processes. 3DNEPH (1970–1983) and RTNEPH (1983–present) cloud-analysis data are available to the scientific community. Civilian users should contact Customer Services, National Climatic Data Center, Federal Building, Asheville, NC 28801; telephone (704) 259-0682. Military users should contact the U.S. Air Force Environmental Technical Applications Center, Federal Building, Asheville, NC 28801-2723; telephone (704) 259-0224.

Acknowledgments. The 3DNEPH and RTNEPH have evolved over the years, and the current improvements are possible only due to the considerable effort of previous model caretakers. A short, and certainly incomplete, list of nephanalysts at AFGWC over the decades include Al Coburn, Jim Conry, William Cox, Jim Cramer, Pat Freeman, Falko Fye, Randy Horlocker, Jim Ingle, Bill Irvin, Paul Janota, Jeff Koenig, Ray Kiess, Tom Lee, Saba A. Luces, Dan Pophin, Gerald Sikula, Jim Stefano, Frank Tower, Ronald

Wachtmann, Tom Walters, Nick Wilde, and the current caretaker, Capt. Norman Mandy. For past AFGWC nephanalysts left off the list, our apologies for not recognizing your hard work, too.

Many people carefully reviewed this manuscript, including Norman Mandy, Dan Pophin, Ray Kiess, and Jim Cramer at AFGWC, and Thomas Nehrkorn, Marina Zivkovic, Gary Gustafson, and Ron Isaacs at AER. Gary Gustafson and Joan Ward helped with the production of figures.

We give special thanks to Ken Mitchell at NMC for his especially thorough review and helpful suggestions.

Part of the preparation of this manuscript was supported by DoD contract F19628-91-C-0011.

REFERENCES

Allen, R. C., P. Durkee, and C. Wash, 1990: Snow/cloud discrimination with multispectral satellite measurements. *J. Appl. Meteor.*, **29,** 994–1004.

Campana, K. A., K. E. Mitchell, S. K. Yang, Y. Hou, and L. L. Stowe, 1991: Validation and improvement of cloud parameterization at the National Meteorological Center. Preprints, *9th Conf. Num. Wea. Pred.*, Denver, Amer. Meteor. Soc., 131–134.

Coakley, J. A., and F. Bretherton, 1982: Cloud cover from high resolution scanner data: Detecting and allowing for partially filled fields of view. *J. Geophys. Res.*, **87,** 4917–4932.

Crum, T. D., 1987: AFGWC cloud forecast models. AFGWC Tech. Note 87/001. Air Force Global Weather Central, 73 pp.

d'Entremont, R. P., 1986: Low- and mid-level cloud analysis using nighttime multispectral imagery. *J. Climate Appl. Meteor.*, **25,** 1853–1869.

——, R. S. Hawkins, and J. T. Bunting, 1982: Evaluation of automated imagery algorithms for use in the Three-Dimensional Nephanalysis Model at AFGWC. AFGL-TR-82-0397, Phillips Laboratory/Geophysics Directorate, Hanscom AFB, MA, 39 pp.

——, J.-L. Moncet, T. R. Miller, M. K. Griffin, L. W. Thomason, J. T. Bunting, and C. B. Schaaf, 1989: An outline for the RTNEPH infrared water vapor attenuation study. GL-TR-89-0344, Phillips Laboratory/Geophysics Directorate, Hanscom AFB, MA, 50 pp.

Ek, M., and L. Mahrt, 1989: A User's Guide to OSU1DPBL Version 1.0.3, A One-Dimensional Planetary Boundary Layer Model (Draft). Dept. of Atmos. Sci., Oregon State University, 190 pp.

Fye, F. K., 1978: The AFGWC automated cloud analysis model. AFGWC Tech. Note 78/002, Air Force Global Weather Central. Offutt AFB, NE, 97 pp.

Hall, S. J., 1986: The AFGWC snow analysis model. AFGWC Tech. Note 86/001, AFGWC, Offutt AFB, NE, 23 pp.

Hawkins, R. S. 1980: A clustering technique for satellite image analysis. Preprints, *8th Conf. Wea. Fcst. and Anal.*, Denver, Amer. Meteor. Soc., 115–118.

Heinrichs, J. F., A. Koscielny, and R. Savage, 1990: A statistical surface type classifier for SSM/I data. Preprints, *5th Conf. Satellite Meteor. and Ocean.*, London, Amer. Meteor. Soc., 257–261.

Henderson-Sellers, A., 1986: Layer cloud amounts for January and July 1978 from 3D-Nephanalysis. *J. Climate Appl. Meteor.*, **25,** 118–132.

Hoke, J. E., L. L. Hayes, and L. G. Renninger, 1981: Map projections and grid systems for meteorological applications. AFGWC Tech. Note 79/003, AFGWC, Offutt AFB, NE, 86 pp.

Kiess, R. B., and W. Cox, 1988: The AFGWC automated real-time cloud analysis model. AFGWC Tech. Note 88/001, Air Force Global Weather Central, Offutt AFB, NE, 82 pp.

Lejenas, H., 1979: Initialization of moisture in primitive equation models. *Mon. Wea. Rev.*, **107,** 1299–1305.

Mahrt, L., and H. Pan, 1984: A two-layer model of soil hydrology. *Bound.-Layer Meteor.*, **29,** 1–20.

Minnis, P., 1989: Viewing angle dependence of cloudiness determined from coincident GOES East and GOES West data. *J. Geophys. Res.*, **89,** 4987–4996.

Mitchell, K. E., and D. Hahn, 1989: Development of a cloud forecast scheme for the GL baseline global spectral model. GL-TR-89-0343, Phillips Laboratory/Geophysics Directorate, Hanscom AFB, MA, 147 pp.

Mohanty, U. C., A. Kasahara, and R. Errico, 1986: The impact of diabatic heating on the initialization of a global forecast model. *J. Meteor. Soc. Jpn.*, **64,** 805–817.

Nehrkorn, T. R., and R. N. Hoffman, 1990: Inferring humidity profiles from 3DNEPH data. *J. Appl. Meteor.*, **29,** 1330–1343.

Norquist, D. C., 1988: Alternative forms of humidity information in global data assimilation. *Mon. Wea. Rev.*, **116,** 452–471.

Rossow, W. B., E. Kinsella, A. Wolf, and L. Gardner, 1985: International Satellite Cloud Climatology Project (ISCCP) description of reduced resolution radiance data. WMO/TD No. 58, World Meteorological Organization, 132 pp.

Saunders, R. W., and K. Kriebel, 1988: An improved method for detecting clear sky and cloudy radiances from AVHRR data. *Intl. J. Rem. Sens.*, **9,** 123–150.

Schiffer, R. A., and W. Rossow, 1985: ISCCP global radiance dataset: A new resource for climate research. *Bull. Amer. Meteor. Soc.*, **66,** 1498–1505.

Schlatter, T. W., 1975: Some experiments with a multivariate statistical objective analysis scheme. *Mon. Wea. Rev.*, **103,** 246–257.

Schneider, S. H., 1972: Cloudiness as a global climate feedback mechanism: The effects on the radiative balance and surface temperature of variations in cloudiness. *J. Atmos. Sci.*, **29,** 1413–1422.

Slingo, J. M., 1987: The development and verification of a cloud prediction scheme for the ECMWF model. *Quart. J. Roy. Meteor. Soc.*, **113,** 899–927.

Snow, J. W., 1990: Modeling the variation of cloud cover with viewing angle using space shuttle cloud imagery. GL-TR-90-0130, Phillips Laboratory/Geophysics Directorate, Hanscom AFB, MA, 50 pp.

Sundqvist, H., E. Berge, and J. Kristjansson, 1989: Condensation and cloud parameterization studies with a mesoscale numerical weather prediction model. *Mon. Wea. Rev.*, **117,** 1641–1657.

Taylor, V. R., and L. Stowe, 1984: Reflectance characteristics of uniform earth and cloud surfaces derived from *NIMBUS-7* ERB. *J. Geophys. Res.*, **89,** 4987–4996.

Weinreb, M. P., and M. L. Hill, 1980: Calculation of atmospheric radiances and brightness temperatures in infrared window channels of satellite radiometers. NOAA Tech. Rep. NESS 80, U.S. Department of Commerce, Washington, D.C., 40 pp.

Wielicki, B. A., and R. Welch, 1986: Cumulus cloud properties derived using Landsat data. *J. Climate Appl. Meteor.*, **25,** 261–276.

Zamiska, A., 1986: RTNEPH USAFETAC Climatic Database Users Handbook No. 1. USAFETAC/User Handbook—86/001, USAF Environmental Technical Applications Center, Operating Location A, Asheville, N.C., 15 pp.